Article

Collector Efficiency in Downward-Type Double-Pass Solar Air Heaters with Attached Fins and Operated by External Recycle

Ho-Ming Yeh and Chii-Dong Ho *

Energy and Opto-Electronic Materials Research Center, Department of Chemical and Materials Engineering, Tamkang University, Tamsui, New Taipei 251, Taiwan;
E-Mail: hmyeh@mail.tku.edu.tw

*   Author to whom correspondence should be addressed; E-Mail: cdho@mail.tku.edu.tw;
    Tel.: +886-2-26215656 (ext. 2724); Fax: +886-2-26209887.

Abstract: The collector efficiency in a downward-type double-pass external-recycle solar air heater with fins attached on the absorbing plate has been investigated theoretically. Considerable improvement in collector efficiency is obtainable if the collector is equipped with fins and the operation is carried out with an external recycle. Due to the recycling, the desirable effect of increasing the heat transfer coefficient compensates for the undesirable effect of decreasing the driving force (temperature difference) of heat transfer, while the attached fins provide an enlarged heat transfer area. The order of performances in the devices of same size is: double pass with recycle and fins > double pass with recycle but without fins > single pass without recycle and fins.

Nomenclature:

A_c	surface area of the absorbing plate, BL (m²)
B	the width of absorber surface area, nw_1 (m)
C_p	specific heat of air at constant pressure (J/kg K)
D_e	equivalent diameter of the channel (m)
E	further improvement in collector efficiency
F'	efficiency factor of the solar air heater

F_R	heat-removal factor for the solar air heater
H	height of the air tunnel in the solar collector, or the distance between glass cover and absorbing plate (m)
h	convective feat-transfer coefficient for fluid flowing over the plate of duct (W/m^2 K)
h_{p-R}	radiant heat-transfer coefficient between two parallel plates (W/m^2 K)
h_w	convective heat-transfer coefficient between glass cover and ambient (W/m^2 K)
I	improvement in collector efficiency in the device without fins
I_f	improvement in collector efficiency in the device with fins attached
I_o	solar radiation incident (W/m^2)
k	thermal conductively of air (W/m K)
k_s	thermal conductivity of absorbing plate and fins (W/m K)
L	collector length (m)
$\dot{m}$	mass flow-rate of air (kg/s)
M	quantity defined by Equation (6)
n	fin number
Nu	Nusselt number
Q_u	useful gain of energy carried away by air per unit time (W)
R	reflux ratio
Re	Reynolds number of flow channel
T	temperature (K)
t	fin thickness (m)
U_t	loss coefficient from the top of solar collector to the ambient (W/m^2 K)
$\bar{v}$	average air velocity in the flow channel (m/s)
V	wind velocity (m/s)
w_1	distance between fins (m)
w_2	height of fin (m)
z	axis along the flow direction (m)

Greek Letters

η	collector efficiency
σ	the Stefan–Boltzmann constant (W/m^2 K^4)
ε_g	emissivity of glass cover
ε_p	emissivity of absorbing plate
ε_R	emissivity of bottom plate
τ_g	transmittance of glass cover
ϕ	dimensionless quantity defined by Equation (4)
α_p	absorptivity of the absorbing plate

Subscripts

a	ambient
f	fluid
i	inlet
m	mean value
o	outlet at subchannel 2 ($z = 0$), or single-pass operation without recycle
p	absorbing plate
R	bottom plate
1,2	subchannel 1, subchannel 2

Superscripts

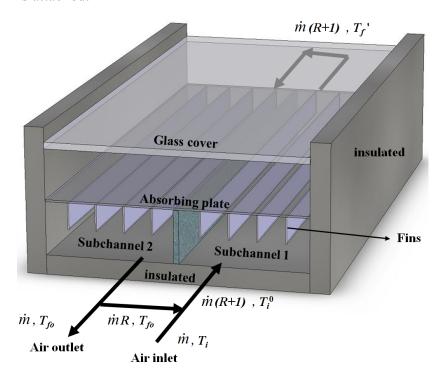|	
0	mixed
'	outlet at the first pass or inlet at subchannel 2 ($z = L$)

1. Introduction

In addition to the essential effects of free and forced convections [1–3], considerable improvement in collector efficiency is also achievable by attaching fins to increase the heat transfer area [1,4], and by using baffles [5], or the matrix [6] to create the turbulent inside the flow channel. It was pointed out that applications of multi-pass [7–9] or recycle operation [10–16] can effectively enhance the performances of heat and mass transfer due to the increase in fluid velocity. The effect of external recycle on the performances in the single-pass [17] and double-pass [18] solar air heaters has been investigated. Considerable improvement in collector efficiency is obtainable if the operation is carried out with an external recycle, where the desirable effect of increasing fluid velocity can generally compensate for the undesirable effect of decrease in heat-transfer driving force (temperature difference) due to remixing by recycle operation. It is the purpose of this work to further investigate the performance in a downward-type double-pass external-recycle solar air heater with fins attached on the absorbing plate.

2. Theoretical Analysis

Consider a recycling double-pass solar air heater with n fins attached on the absorbing plate, as shown in Figure 1. The width, length and height of the flow channel are *B*, *L* and *H*, respectively. An insulated plate with negligible thickness is placed vertical to the absorbing plate and bottom plate, at the centerline to divide the flow channel into subchannel 1 and subchannel 2 of equal width *B*/2, and that a pump is installed for recycle with reflux ratio *R*. For a double-pass operation with external recycle, before entering subchannel 1, the airflow with mass flow rate $\dot{m}$ and inlet airflow temperature T_i will mix with part of the airflow exiting from subchannel 2 with mass flow rate $\dot{m}R$ and outlet airflow temperature T_{fo}. The following assumptions are made in the analysis: (1) the absorbing-plate, bottom-plate and bulk-fluid temperatures are functions of the flow direction (z) only; (2) both glass cover and fluid do not absorb radiant energy; (3) except the glass cover, all parts of the outside surface

of solar air collector, as well as the thin plate for separation subchannels 1 and 2, are well thermally insulated; (4) the physical properties of the fluid and materials are constant; and (5) steady state operation.

Figure 1. Schematic diagram of a downward-type double-pass external-recycle solar air heater with fins attached.

2.1. Temperature Distribution for the Fluid in Subchannel 1

The steady-state energy balance for a differential section of the absorbing plate with n fins attached, bottom plate and flowing fluid are, respectively:

$$I_0 \tau_g \alpha_p (B/2)dz = h\phi(B/2)dz(T_p - T_{f1}) + h_{r,p-R}(B/2)dz(T_P - T_R) + U_t(B/2)dz(T_p - T_a) \qquad (1)$$

$$h_{r,p-R}(B/2)dz(T_P - T_R) = h(B/2)dz(T_R - T_{f1}) \qquad (2)$$

$$[\dot{m}(1+R)C_p](\frac{dT_{f1}}{dz})dz = h\phi(B/2)dz(T_p - T_{f1}) + h(B/2)dz(T_R - T_{f1}) \qquad (3)$$

where:

$$\phi = 1 + (A_f/A_c)\eta_f \qquad (4)$$

in which A_f (= $2nw_2L$) and A_c (= BL) are the surface areas of fins and absorbing plate, respectively, while η_f denotes the fin efficiency [19], *i.e.*:

$$\eta_f = (\tanh Mw_2)/Mw_2 \qquad (5)$$

and:

$$M = \sqrt{2h/k_s t} \qquad (6)$$

where w_2 and k_s are the height of a fin and thermal conductivity of the absorbing plate and fins, respectively, while t is the fin thickness.

Solving Equations (1) and (2) for $(T_p - T_{f1})$ and $(T_R - T_{f1})$:

$$T_p - T_{f1} = \frac{I_0 \tau_g \alpha_p (h + h_{r,p-R}) - (hU_t + h_{r,p-R}U_t)(T_{f1} - T_a)}{h\phi(h + h_{r,p-R}) + h(h_{r,p-R} + U_t) + h_{r,p-R}U_t} \tag{7}$$

$$T_R - T_{f1} = \frac{I_0 \tau_g \alpha_p h_{r,p-R} - h_{r,p-R}U_t(T_{f1} - T_a)}{h\phi(h + h_{r,p-R}) + h(h_{r,p-R} + U_t) + h_{r,p-R}U_t} \tag{8}$$

The detailed explanation in the derivations of Equations (7) and (8) are expressed mathematically and shown in Appendix. Substituting Equations (7) and (8) into Equation (3), we have:

$$[2\dot{m}(1 + R)C_P)]\frac{dT_{f1}}{dz} = BF'[I_0 \tau_g \alpha_p - U_t(T_{f1} - T_a)] = 0 \tag{9}$$

where:

$$F' = \frac{h\phi(h + h_{r,p-R}) + hh_{r,p-R}}{h\phi(h + h_{r,p-R}) + h(h_{r,p-R} + U_t) + h_{r,p-R}U_t} \tag{10}$$

in which F' is called collector efficiency factor, which is essential constant for any design and fluid flow rate [20], and U_t is the loss coefficient from the top of the solar collector to the ambient. If U_t is assumed to be constant along the flow direction, Equation (9) can be easily integrated for the boundary condition:

$$T_{f1} = T_i^0 \text{ at } z = 0 \tag{11}$$

The result is:

$$\frac{T_{f1} - T_a - (I_0 \tau_g \alpha_p / U_t)}{T_i^0 - T_a - (I_0 \tau_g \alpha_p / U_t)} = \exp\left[-\frac{F'U_t Bz}{2\dot{m}(1 + R)C_p}\right] \tag{12}$$

Equation (12) is the temperature distribution of the bulk fluid along the flow direction of subchannel 1. Thus, the fluid temperature at the outlet of subchannel 1 is readily obtained from Equation (12) by substituting the condition: $T_{f1} = T'_f$ at $z = L$. The result is:

$$\frac{T'_f - T_a - (I_0 \tau_g \alpha_p / U_t)}{T_i^0 - T_a - (I_0 \tau_g \alpha_p / U_t)} = \exp\left[-\frac{F'U_t A_c}{2\dot{m}(1 + R)C_p}\right] \tag{13}$$

where $A_c = BL = nw_1L$, surface area of the absorbing plate.

2.2. Temperature Distribution for the Fluid in Subchannel 2

The differential energy-balance equation for the fluid in subchannel 2 is readily obtained by following the same procedure from Equation (1) through Equation (13) with T_{f1} and (dT_{f1}/dz) replaced by T_{f2} and $-(dT_{f2}/dz)$, respectively. The result is:

$$-[2\dot{m}(1 + R)C_p]\frac{dT_{f2}}{dz} = BF'[I_0 \tau_g \alpha_p - U_t(T_{f2} - T_a)] \tag{14}$$

Integrating Equation (14) with the use of the boundary condition:

$$T_{f2} = T_{fo} \text{ at } z = 0 \tag{15}$$

one has the temperature distribution for the fluid in subchannel 2 as:

$$\frac{T_{f2} - T_a - (I_0 \tau_g \alpha_p / U_t)}{T_{fo} - T_a - (I_0 \tau_g \alpha_p / U_t)} = \exp\left[\frac{F'U_t Bz}{2\dot{m}(1+R)C_p}\right] \tag{16}$$

Thus, in addition to Equation (13), the fluid temperature T'_f at the inlet of subchannel 2 ($z = L$) is also obtained from Equation (16) by substituting $z = L$ and $T_{f2} = T'_f$. The result is:

$$\frac{T'_f - T_a - (I_0 \tau_g \alpha_p / U_t)}{T_{fo} - T_a - (I_0 \tau_g \alpha_p / U_t)} = \exp\left[\frac{F'U_t A_c}{2\dot{m}(1+R)C_p}\right] \tag{17}$$

2.3. Collector Efficiency and Fluid Outlet Temperature

The fluid outlet temperature is readily obtained by combining Equations (13) and (17) to eliminate T'_f as:

$$\frac{T_{fo} - T_a - (I_0 \tau_g \alpha_p / U_t)}{T_i^0 - T_a - (I_0 \tau_g \alpha_p / U_t)} = \exp\left[-\frac{F'U_t A_c}{\dot{m}(1+R)C_p}\right] \tag{18}$$

Two different expressions for the useful again of energy Q_u carried away by air can be obtained as:

$$Q_u = \dot{m}C_p(T_{fo} - T_i) \tag{19}$$

$$= \dot{m}(1+R)C_p(T_{fo} - T_i^0) \tag{20}$$

Inspection of Equation (19) shows that the mixed inlet temperature T_i^0 due the recycle is not specified a prior. The relation for the mixing effect at the inlet in Equation (20) was used for determination of this value. Thus, a combination of Equations (19) and (20) gives:

$$T_i^0 = T_{fo} - (T_{fo} - T_i)/(1+R) = T_i + [R/(1+R)](T_{fo} - T_i) \tag{21}$$

The collector efficiency may be defined as:

$$\eta_{cf} = \frac{Q_u}{I_0 A_c} = [\dot{m}(1+R)C_p / I_0 A_c](T_{fo} - T_i^0) \tag{22}$$

or

$$\eta_{cf} = \dot{m}C_p(T_{fo} - T_i)/I_0 A_c \tag{23}$$

Substitution of Equation (18) into Equation (22) gives:

$$\eta_{cf} = \frac{\dot{m}(1+R)C_p}{I_0 A_c}\{[T_a + (I_0 \tau_g \alpha_p / U_t) - T_i^0]$$

$$+ [T_i^0 - T_a - (I_0 \tau_g \alpha_p / U_t)]\exp[-A_c F'U_t / \dot{m}(1+R)C_p]\} \tag{24}$$

$$= F_R[\tau_g \alpha_p - U_t(T_i^0 - T_a)/I_0]$$

where the heat-removal factor for solar air heater is defined as:

$$F_R = [\dot{m}(1+R)C_p / A_c U_t]\{1 - \exp[-A_c F' U_t / \dot{m}(1+R)C_p]\} \tag{25}$$

Substitution of Equation (21) into Equation (24) with the aid of Equation (18) to eliminate T_i^0 and T_{fo} yields:

$$\eta_{cf} = \frac{F_R[\tau_g \alpha_p - U_t(T_i - T_a)/I_0]}{1 + (F_R U_t A_c / \dot{m}C_p)[R/(1+R)]} \tag{26}$$

Once the collector efficiency is determined, the fluid outlet temperature is readily obtainable from Equation (23), *i.e.*:

$$T_{fo} = T_i + (\eta_{cf} I_0 A_c / \dot{m}C_p) \tag{27}$$

2.4. Mean Fluid and Absorbing-Plate Temperatures

The mean fluid and absorbing-plate temperatures are needed for calculating the heat-transfer coefficients. The mean-fluid temperature may be defined as:

$$T_{fm} = \frac{1}{2L}\int_0^L (T_{f1} + T_{f2})dz \tag{28}$$

Substituting Equations (12) and (16) into Equation (28) and integrating, we have:

$$\begin{aligned}
T_{fm} = \frac{\dot{m}(1+R)C_p}{F'U_t A_c}&\left\{\left(T_i^0 - T_a - \frac{I_0 \tau_g \alpha_p}{U_t}\right)\left[1 - \exp\left(-\frac{F'U_t A_c}{2\dot{m}(1+R)C_p}\right)\right]\right.\\
&\left. + \left(T_{fo} - T_a - \frac{I_0 \tau_g \alpha_p}{U_t}\right)\left[\exp\left(\frac{F'U_t A_c}{2\dot{m}(1+R)C_p}\right) - 1\right]\right\} + \left(T_a + \frac{I_0 \tau_g \alpha_p}{U_t}\right)
\end{aligned} \tag{29}$$

With the use of Equations (23) and (24) to eliminate T_{fo} and T_i^0, respectively, T_{fm} in Equation (29) can be expressed in term of η_{cf} as:

$$\begin{aligned}
T_{fm} = \frac{\dot{m}(1+R)C_p}{F'U_t A_c}&\left\{\left(\frac{I_0 \eta_{cf}}{F_R U_t}\right)\left[\exp\left(-\frac{F'U_t A_c}{2\dot{m}(1+R)C_p}\right) - 1\right]\right.\\
&\left. + \left[\left(\frac{\eta_{cf} I_0 A_c}{\dot{m}C_p}\right) + \left(T_i - T_a - \frac{I_0 \tau_g \alpha_p}{U_t}\right)\right]\left[\exp\left(\frac{F'U_t A_c}{2\dot{m}(1+R)C_p}\right) - 1\right]\right\} + \left(T_a + \frac{I_0 \tau_g \alpha_p}{U_t}\right)
\end{aligned} \tag{30}$$

The mean absorbing-plate temperature may be defined in term η_{cf} as:

$$\eta_{cf} = \tau_g \alpha_p - U_t(T_{pm} - T_a)/I_0 \tag{31}$$

or:

$$T_{pm} = T_a + (I_0/U_t)(\tau_g \alpha_p - \eta_{cf}) \tag{32}$$

Equations (30) and (32) are the expressions of T_{fm} and T_{pm} in terms of η_{cf}.

2.5. Heat-Transfer Coefficients

The convective heat-transfer coefficient h_w for air flowing over the outside surface of the glass cover depends primarily on the wind velocity V. McAdams [21] obtained the experimental result as:

$$h_w = 5.7 + 3.8\,V \tag{33}$$

An empirical equation for the loss coefficient from the top of the solar collector to the ambient U_L was developed by Klein [22] following the basic procedure of Hottel and Woertz [23]. For the horizontal collector shown in Figure 1:

$$U_t = \left\{ \dfrac{T_{pm}/520}{\left[\dfrac{(T_{pm}-T_a)}{1+(1+0.089h_w-1.1166h_w\varepsilon_p)(1+0.07866)} \right]^{0.43(1-100/T_{pm})}} + \dfrac{1}{h_w} \right\}^{-1}$$
$$+ \dfrac{\sigma(T_{pm}-T_a)(T_{pm}^2+T_a^2)}{\dfrac{1}{(\varepsilon_p 0.00591h_w)} + \dfrac{2+(1+0.089h_w-0.1166h_w\varepsilon_p)(1+0.07866)-1+0.133\varepsilon_p}{\varepsilon_g} - 1} \tag{34}$$

The radiation coefficient between the two air-duct surfaces may be estimated by assuming a mean radiant temperature equal to the mean fluid temperature [20]:

$$h_{r,p-R} = \dfrac{4\sigma T_{fm}^3}{\dfrac{1}{\varepsilon_p} + \dfrac{1}{\varepsilon_R} - 1} \tag{35}$$

In the study of solar air heaters and collector-storage walls, it is necessary to know the forced convection heat-transfer coefficient between two flat plates. For air, the following correlation may be derived from Kays' data for fully developed turbulent flow with one side heated and the other side insulated [24]:

$$\text{Nu} = hD_e/k = 0.0158\,\text{Re}^{0.8} \tag{36}$$

where the equivalent diameter of the ducts are:

$$D_{e,1} = D_{e,2} = \dfrac{4(HB/2)}{2(H+B/2)} = \dfrac{2HB}{2H+B} \tag{37}$$

and the average air velocities in subchannels 1 and 2 for double-pass operation are:

$$\overline{v_1} = \overline{v_2} = \dfrac{2\dot{m}(1+R)}{HB\rho} \tag{38}$$

Thus, from Equations (37) and (38), one obtains the Reynolds numbers for the rectangular ducts as:

$$\text{Re}_1 = \text{Re}_2 = \dfrac{4\dot{m}(1+R)}{\mu(2H+B)} \tag{39}$$

2.6. Calculation Method for η_{cf} and T_{fo}

The calculation of prediction values for collector efficiency and outlet fluid temperature is now described as follows. First, with known collector geometries (L,B,H) and system properties $(\tau_g, \alpha_p, C_p, \rho, \mu, k, k_s, \varepsilon_p, \varepsilon_g, \varepsilon_R)$, as well as the given operating conditions $(I_0, T_a, V, \dot{m}, R, T_i, n)$, a temporary value of η_{cf} is estimated from Equation (26) once T_{fm} and T_{pm} are assumed. The values of T_{fm} and T_{pm} are then checked by using Equations (30) and (32), respectively, and new values of T_{fm} and T_{pm} may be obtained. If the calculated values for T_{fm} and T_{pm} are different from the assumed values, continued calculations by iteration is needed until the last assumed values meet the finally calculated values, and thus the corresponding value for η_{cf} is also finally obtained. Once the correct value of η_{cf} is obtained, the outlet fluid temperature is readily calculated from Equation (27).

The following flow sheet may be helpful for simply expressing the calculation procedure:

$$\text{Given} \begin{cases} \tau_g, \alpha_p, C_p, \rho, \mu, k, k_s, \varepsilon_p, \varepsilon_g, \\ \varepsilon_R, I_0, T_a, V, \dot{m}, R, T_{f,i}, n \end{cases} \xrightarrow[\text{Equation (26)}]{\text{with } T_{fm} \text{ and } T_{pm} \text{ assumed}} \eta_{cf} \xrightarrow[\text{Equation (32)}]{\text{Equation (30)}} \begin{matrix} T_{fm} \\ T_{pm} \end{matrix} \xrightarrow[\text{Equation (27)}]{\text{Equation (20)}} \begin{matrix} Q_u \\ T_{fo} \text{ and } \eta_{cf} \end{matrix} \quad (40)$$

$$\text{iterations}$$

3. Results and Discussion

3.1. Numerical Example

The improvement in performance of an external-recycle double-pass solar air heater with n fins attached on the absorbing plate may be illustrated numerically by using Table 1 and the following design and operating conditions: $L = B = 0.6$ m; $A_c = LB = 0.36$ m^2; $H = 0.05$ m; $w_1 = 0.05$ m; $w_2 = 0.02$ m; $t = 0.001$ m; $k_s = 45$ W/mK; $n = 12$; $\tau_g = 0.875$; $\alpha_p = 0.95$; $\varepsilon_g = 0.94$; $\var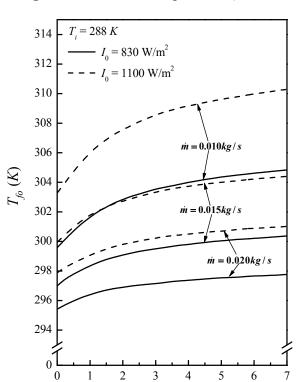epsilon_p = 0.95$; $\varepsilon_R = 0.94$; $I_0 = 830$ and 1100W/m^2; $T_i = 288, 293$ and 298 K; $V = 1$ m/s; $\dot{m} = 0.01, 0.015$ and 0.02 kg/s; $T_a = 283$ K, $\sigma = 5.67 \times 10^{-8}$ W/m^2 K^4.

Table 1. Physical properties of air at 1 atm [20].

T (K)	ρ (kg/m^3)	C_p (J/kg K)	k (W/m K)	μ (kg/m s)
273	1.292	1006	0.0242	1.72×10^{-5}
293	1.204	1006	0.0257	1.81×10^{-5}
313	1.127	1007	0.0272	1.90×10^{-5}
333	1.059	1008	0.0287	1.99×10^{-5}
353	0.999	1010	0.0302	2.09×10^{-5}

By substituting the specified values into the appropriate equations with the use of Table 1 for the physical properties of air, theoretical predictions for collector efficiency and outlet air temperature were obtained.
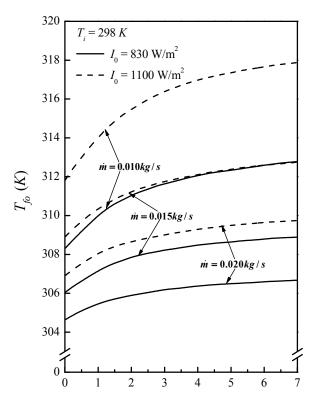
3.2. Effects of Operating Parameters on Collector Efficiency

As might be expected, the outlet air temperature T_{fo} increases with the inlet air temperature T_i, resulting in decrease in collector efficiency η_{cf}.
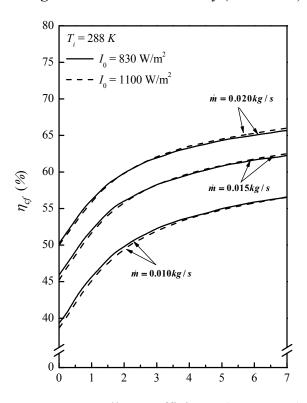
Figure 2. Air outlet temperature ($T_i = 288$ K).

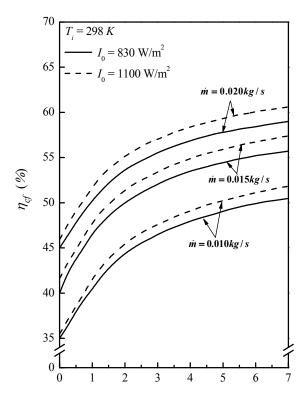**Figure 3.** Air outlet temperature ($T_i = 298$ K).

Figure 4. Collector efficiency ($T_i = 288$ K).

Figure 5. Collector efficiency ($T_i = 298$ K).

On the other hand, the outlet air temperature decreases when the air flow rate $\dot{m}$ increases in which the collector efficiency increases. Of course, both the outlet air temperature and collector efficiency increase when the solar radiation incident I_0 increases. These results are shown in Figures 2–5.

3.3. Improvement in Performance by Recycling

The improvements I_f and I in collector efficiencies (η_{cf} and η_c) by using the double pass recycled collectors with and without fins attached are best illustrated by calculating the percentage increase in collector efficiency based on η_0 obtained in the single-pass device of same size, operated without recycling and fins attached, *i.e.*:

$$I_f = \frac{\text{collector efficiency of double} - \text{pass recycled device with fins } \eta_{cf}}{\text{collector efficiency of single} - \text{pass device without recycling and fins } \overline{\eta}_c} - 1 \qquad (41)$$

$$I = \frac{\text{collector efficiency of double} - \text{pass recycled device without fins } \eta_c}{\text{collector efficiency of single} - \text{pass device without recycling and fins } \overline{\eta}_c} - 1 \qquad (42)$$

The theoretical values of I_f for the system of present interest with the given values of η_0 [17], were calculated using Equation (41), and the results are listed in Table 2. The predicted values for I without fins were already calculated in the previous work [18], and the results are also presented in Table 2 for comparison. From this table and Figures 2–5, we see that operating with recycling substantially improves the collector efficiency either with or without fins attached. The improvements increase with increasing reflux ratio R, especially when operating at lower air flow rate $\dot{m}$ with higher inlet air temperature T_i. For instances, the improvements of collector efficiency I_f in the double-pass recycled collector with fins attached and operating at $\dot{m} = 0.01\,\text{kg/s}$, $T_i = 298$ K and $R = 5$, are 123.49% and 129.54%, respectively, for $I_0 = 830$ and 1100 W/m^2. It is concluded that the contribution of the desirable effect of increasing fluid velocity by applying the external-recycle operation may be more effective than the undesirable effect of lowering the temperature difference.

Table 2. The improvement of performance for: (**a**) $I_0 = 830$ W/m^2; (**b**) $I_0 = 1100$ W/m^2.

	T_i (K)	$\dot{m}$ (kg/s)	$\overline{\eta}_c$ (%)	I_f (%)				I (%)			
				$R=0$	$R=1$	$R=3$	$R=5$	$R=0$	$R=1$	$R=3$	$R=5$
(a)	288	0.01	24.60	58.94	88.30	111.92	123.02	36.49	68.91	97.68	111.97
		0.015	30.35	50.37	73.58	91.67	99.99	31.04	57.63	80.42	91.90
		0.02	34.65	44.47	63.88	78.66	85.35	27.32	50.30	69.63	79.00
	293	0.01	23.28	58.94	88.40	119.22	123.34	36.52	69.34	97.93.	112.71
		0.015	28.75	50.41	73.76	92.01	100.42	31.10	58.08	80.90	92.56
		0.02	32.84	44.50	64.07	79.02	85.79	27.40	50.67	70.29	79.82
	298	0.01	21.96	58.85	88.39	112.26	123.49	36.51	69.40	98.25	112.82
		0.015	27.14	50.30	73.77	92.15	100.63	31.12	58.09	81.16	93.01
		0.02	31.02	44.41	64.11	79.20	86.05	27.42	50.69	70.30	79.95
(b)	288	0.01	23.92	61.21	92.15	117.08	119.03	36.49	68.85	97.53	111.77
		0.015	29.73	52.32	76.71	95.70	104.45	31.04	57.63	80.28	91.70
		0.02	34.11	46.09	66.39	81.85	88.85	27.32	50.23	69.48	78.82
	293	0.01	22.90	61.29	92.34	117.39	129.17	36.52	69.19	97.61	112.27
		0.015	28.48	52.42	83.39	96.01	104.92	31.10	57.94	80.60	92.15
		0.02	32.69	46.25	66.71	82.33	89.41	27.40	50.52	69.98	79.42
	298	0.01	21.87	61.38	92.52	117.69	129.54	36.51	69.17	97.75	112.16
		0.015	27.21	52.58	77.23	96.52	105.43	31.12	57.88	80.70	92.37
		0.02	31.26	46.33	66.92	82.69	89.85	27.42	50.49	69.86	79.38

3.4. Effect of Fin Attached on Device Performance

The improvements *I* in collector efficiency obtained in a double-pass recycled solar air heater of the same size but without fins attached [18], are also listed in Table 2 for comparisons. It is seen that considerable further enhancement of collector efficiency is achieved if fins are attached on the absorbing plate for increasing the heat transfer area. Taking the case of $T_i = 298$ K, $\dot{m} = 0.01\,\text{kg/s}$, $I_0 = 1100$ W/m^2 and $R = 1$ for example, more than 23% improvement ($I_f - I = 92.52 - 69.17\%$) is obtained when employing the recycled double-pass collector with fins attached, instead of using the same device but without fins, which was employed in the previous work [18]. The further enhancement in collector efficiency E by attaching fins on the absorbing plate may be illustrated, based on the device of same size but without recycle, as:

$$E = \frac{\eta_{cf} - \eta_c}{\eta_c} \tag{43}$$

Equation (43) may be rewritten using Equations (41) and (42) as:

$$E = \left[\frac{(\eta_{cf} - \overline{\eta}_c) - (\eta_c - \overline{\eta}_c)}{\overline{\eta}_c}\right](\overline{\eta}_c / \eta_c) = (I_f - I)(\overline{\eta}_c / \eta_c) \tag{44}$$

$$= \frac{I_f - I}{1 + I} \tag{45}$$

Some values of *E* were calculated from Table 2, and the results are listed in Table 3. As seen this table, the further enhancement of the collector efficiency in the device with fins increases with the solar radiation incident I_0, while decreases when the air flow sate $\dot{m}$ and reflux ratio R increases. The influence of the inlet air temperature T_i on E is not evident.

Table 3. Further enhancement in collector efficiency with fin: (**a**) $I_0 = 830$ W/m^2; (**b**) $I_0 = 1100$ W/m^2.

	T_i (K)	$\dot{m}$ (kg/s)	E (%)			
			$R = 0$	$R = 1$	$R = 3$	$R = 5$
(a)	288	0.01	16.45	11.48	7.20	5.21
		0.015	14.75	10.12	6.24	4.22
		0.02	13.47	9.04	5.32	3.55
	298	0.01	16.37	11.21	7.07	5.01
		0.015	14.63	9.92	6.07	3.95
		0.02	13.33	8.91	5.23	3.39
(b)	288	0.01	18.11	13.80	9.90	7.96
		0.015	16.24	12.10	8.55	6.64
		0.02	14.74	10.76	7.30	5.57
	298	0.01	18.22	13.80	10.08	8.19
		0.015	16.37	12.26	8.75	6.79
		0.02	14.84	10.92	7.55	5.84

4. Conclusions

The performance in a double-pass solar air heater with external recycling was investigated in a previous work [18]. In the present study the absorbing plate of this device is attached with fins for further improved performance. The predicting equation for the useful gain Q_u, the collector efficiency η_{cf} and the outlet air temperature T_{fo}, were derived from the energy balance for the absorbing plate, the bottom plate and flowing air. The calculation of η_{cf}, T_{fo} and Q_u may be generally based on Equations (26), (27) and (20), respectively. The most important assumption is that except for the glass cover, all parts of the outside surface of the solar air collector, as well as the insulated plate for separating two flow channels, are well thermally insulated.

In addition to the double-pass operation with external recycling, further enhancement in collector efficiency is obtainable if the operation is carried out also with fins attached on the absorbing plate. The further enhancement E based on the device without fins, reaches 13.8% for $I_0 = 1100$ W/m^2, $T_i = 298$ K, $\dot{m} = 0.01$ kg/s and $R = 1$. E decreases when the air flow rate and/or the reflux ratio increase. As expected, therefore, employing the fins attached on the absorbing plate, is ineffective when the performance is operated under large reflux ratio with high air flow rate.

The improvements of collector efficiencies, I_f and I, in the recycled devices with and without fins attached, increase with increasing reflux ratio, especially for operating at lower air flow rate. It is shown in Table 2 and Figures 2–5 that the desirable effect of increasing the fluid velocity by recycle operation compensates for the undesirable effect of decreasing driving force (temperature difference) for heat transfer due to the remixing at the inlet. We can see in Table 2 that about 130% improvement I_f in collector efficiency is obtained by employing the recycled double-pass solar air heater with fins attached, based on the single-pass device of same size operated without fins. The order of performances in the devices of same size is: double pass with recycle and fins > double pass with recycle but without fins > single pass without recycle and fins.

Acknowledgments

References

1. Yeh, H.M.; Ting, Y.C. Effects of free convection on collector efficiencies of solar air heaters. *Appl. Energy* **1986**, *22*, 145–155.
2. Yeh, H.M.; Lin, T.T. The effect of collector aspect ratio on the collector efficiency of flat-plate solar air heaters. *Energy* **1995**, *20*, 1041–1047.
3. Forson, F.K.; Nazha, M.A.A.; Rajakaruna, H. Experimental and simulation studies on a single pass, double duct solar air heater. *Energy Convers. Manag.* **2003**, *44*, 1209–1227.
4. Naphon, P. On the performance and entropy generation of the double-pass solar air heater with longitudinal fins. *Renew. Energy* **2005**, *30*, 1345–1357.
5. Yeh, H.M.; Ho, C.D.; Lin, C.Y. Effect of collector aspect ratio on the collector efficiency of upward type baffled solar air heaters. *Energy Convers. Manag.* **2000**, *41*, 971–981.

6. Sharma, V.K.; Sharma, S.; Mahajan, R.B.; Garg, H.P. Evaluation of a matrix solar air heater. *Energy Convers. Manag.* **1990**, *30*, 1–8.

7. Yeh, H.M.; Chen, C.H.; Yeh, T.Y. Influence of channel-width ratio on solvent extraction through a double-pass parallel-plate membrane module. *J. Membr. Sci.* **2004**, *230*, 13–19.

8. Yeh, H.M.; Hung, F.C.; Chen, C.H.; Hung, C.R. Effect of recycle-barrier location on membrane extraction in a parallel-flow rectangular module with internal reflux. *J. Membr. Sci.* **2005**, *60*, 167–177.

9. Yeh, H.M. Effects of reflux and reflux-barrier location on solvent extraction through cross-flow flat-plate membrane modules with internal reflux. *J. Membr. Sci.* **2006**, *269*, 133–141.

10. Korpijarvi, J.; Oinas, P.; Reunaneu, J. Hydrodynamics and mass transfer in airlift reactor. *Chem. Eng. Sci.* **1998**, *54*, 2255–2262.

11. Santacesaria, E.; Di Serio, M.; Iengo, P. Mass transfer and kinetics in ethoxylation spray tower loop reactors. *Chem. Eng. Sci.* **1999**, *54*, 1499–1504.

12. Atwnas, M.; Clark, M.; Lazarova, V. Holdup and liquid circulation velocity in a rectangular air-lift bioreactor. *Ind. Eng. Chem. Res.* **1999**, *38*, 944–949.

13. Yeh, H.M.; Tsai, S.W.; Lin, C.S. A study of the separation efficiency in thermal diffusion column with a vertical permeable barrier. *AIChE J.* **1986**, *32*, 971–980.

14. Yeh, H.M.; Tsai, S.W.; Chiang, C.L. Recycle effects on heat and mass transfer through a parallel-plate channel. *AIChE J.* **1987**, *33*, 1743–1746.

15. Ho, C.D.; Yeh, H.M.; Sheu, W.S. An analytical study of heat and mass transfer through a parallel-plate channel with recycle. *Int. J. Heat Mass Transf.* **1998**, *41*, 2589–2599.

16. Ho, C.D.; Yeh, H.M.; Sheu, W.S. The influence of recycle on double-pass heat and mass transfer through a parallel-plate. *Int. J. Heat Mass Transf.* **1999**, *42*, 1707–1722.

17. Yeh, H.M.; Ho, C.D. Solar Air Heaters with External Recycle. *Appl. Therm. Eng.* **2009**, *29*, 1694–1701.

18. Yeh, H.M.; Ho, C.D. Heat-transfer enhancement of double-pass solar air heaters with external recycle. *Appl. Therm. Eng.* **2011**, *42*, 793–800.

19. Bennett, C.O.; Myers, J.E. *Momentum, Heat and Mass Transfer*, 2nd ed.; McGraw-Hill Inc.: New York, NY, USA, 1974; p. 445.

20. Duffie, J.A.; Beckman, W.A. *Solar Engineering of Thermal Processes*, 2nd ed.; Wiley: New York, NY, USA, 1991.

21. McAdams, W.H. *Heat Transmission*, 3rd ed.; McGraw-Hill: New York, NY, USA, 1954.

22. Klein, S.A. Calculation of flat-plate loss coefficients. *Sol. Energy* **1975**, *17*, 79–80.

23. Hottel, H.C.; Woertz, B.B. Performance of flat-plate solar-heat collector. *Trans. ASME* **1942**, *64*, 91–104.

24. Kays, W.M.; Crawford, M.E. *Convective Heat- and Mass-Transfer*, 2nd ed.; McGraw-Hill: New York, NY, USA, 1980; p. 245.

Appendix

The detailed explanation in the derivations of Equations (7) and (8).

One can rewrite Equations (1) and (2), respectively, as follows:

$$I_0 \tau_g \alpha_p = h\phi(T_p - T_{f1}) + h_{r,p-R}(T_p - T_{f1} + T_{f1} - T_R) + U_t(T_p - T_{f1} + T_{f1} - T_a) \tag{A1}$$

$$h_{r,p-R}(T_p - T_{f1} + T_{f1} - T_R) = h(T_R - T_{f1}) \tag{A2}$$

Rearranging Equations (A1) and (A2) into new expressions, one can obtain, respectively:

$$(h\phi + h_{r,p-R} + U_t)(T_p - T_{f1}) = I_0 \tau_g \alpha_p + h_{r,p-R}(T_R - T_{f1}) - U_t(T_{f1} - T_a) \tag{A3}$$

$$(T_R - T_{f1}) = \frac{h_{r,p-R}}{h_{r,p-R} + h}(T_P - T_{f1}) \tag{A4}$$

or:

$$(T_p - T_{f1}) = \frac{h_{r,p-R} + h}{h_{r,p-R}}(T_R - T_{f1}) \tag{A5}$$

Combination of Equations (A3) and (A4) gives:

$$[h\phi(h + h_{r,p-R}) + h_{r,p-R}(h + h_{r,p-R}) + U_t(h + h_{r,p-R})](T_p - T_{f1})$$

$$= I_0 \tau_g \alpha_p(h + h_{r,p-R}) + h_{r,p-R}^2(T_P - T_{f1}) - U_t(h + h_{r,p-R})(T_{f1} - T_a) \tag{A6}$$

or:

$$(T_p - T_{f1}) = \frac{I_0 \tau_g \alpha_p(h + h_{r,p-R}) - U_t(h + h_{r,p-R})(T_{f1} - T_a)}{h\phi(h + h_{r,p-R}) + h(h_{r,p-R} + U_t) + h_{r,p-R}U_t} \tag{7}$$

Similarly, combination of Equations (A3) and (A5) gives:

$$[h\phi(h + h_{r,p-R}) + h_{r,p-R}(h + h_{r,p-R}) + U_t(h + h_{r,p-R})](T_R - T_{f1})$$

$$= I_0 \tau_g \alpha_p h_{r,p-R} + h_{r,p-R}^2(T_R - T_{f1}) - U_t h_{r,p-R}(T_{f1} - T_a) \tag{A6}$$

or:

$$(T_R - T_{f1}) = \frac{I_0 \tau_g \alpha_p h_{r,p-R} - U_t h_{r,p-R}(T_{f1} - T_a)}{h\phi(h + h_{r,p-R}) + h(h_{r,p-R} + U_t) + h_{r,p-R}U_t} \tag{8}$$